

RFACENET: AN END-TO-END NETWORK FOR ENHANCED PHYSIOLOGICAL SIGNAL EXTRACTION THROUGH IDENTITY-SPECIFIC FACIAL CONTOURS

Dali Zhu, Wenli Zhang, Hualin Zeng, Xiaohao Liu, Long Yang, Jiaqi Zheng

Institute of Information Engineering, Chinese Academy of Sciences, Beijing, China
 School of Cyber Security, University of Chinese Academy of Sciences, Beijing, China
 {zhudali, zhangwenli, zenghualin, liuxiaohao, yanglong, zhengjiaqi}@iie.ac.cn

ABSTRACT

Remote photoplethysmography (rPPG) technique extracts blood volume pulse (BVP) signals from subtle pixel changes in video frames. This study introduces rFaceNet, an advanced rPPG method that enhances the extraction of facial BVP signals with a focus on facial contours. rFaceNet integrates identity-specific facial contour information and eliminates redundant data. It efficiently extracts facial contours from temporally normalized frame inputs through a Temporal Compressor Unit (TCU) and steers the model focus to relevant facial regions by using the Cross-Task Feature Combiner (CTFC). Through elaborate training, the quality and interpretability of facial physiological signals extracted by rFaceNet are greatly improved compared to previous methods. Moreover, our novel approach demonstrates superior performance than SOTA methods in various heart rate estimation benchmarks.

Index Terms— remote photoplethysmography, video preprocessing, heart rate estimation, facial contour

1. INTRODUCTION

The traditional method of extracting heart rate signals via electrocardiogram (ECG) is gradually being replaced by portable, non-contact photoplethysmographic blood pressure measurements. Wherein, remote photovolumetric pulse (rPPG) [1] is a technique for non-invasive acquisition of blood volume pulse (BVP) signals based on skin reflection modeling, which can be further used for the extraction of heart rate and respiration signals. Although mainly using facial video as input, previous solutions, which adopt traditional signal processing techniques [2–7] with heuristic rules and non-end-to-end deep learning [8–12] with complex preprocessing, have failed to integrate with facial contours due to technical limitations. This integration has recently been shown an effectively enhancement for facial BVP signal extraction [13–15].

Despite the significant results, previous works [13–15] tend to introduce unnecessary noises of input information when adding an equivalent number of RGB image frames,

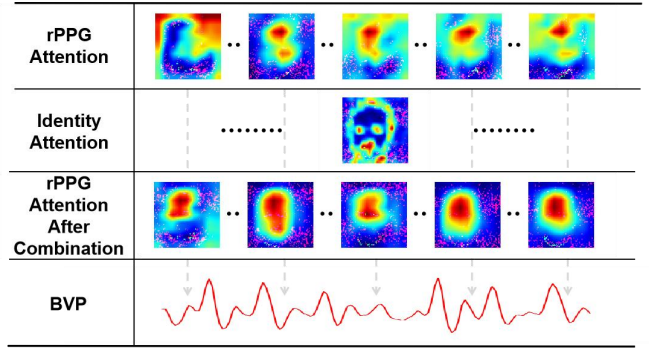


Fig. 1: The rPPG attention region before and after being combined with identity-attention facial contours is shown with Gram-CAM [17].

leading to the efficiency dropping. To minimize the redundancy, we attempt to categorize facial contours based on identity within the slight facial changes from frame to frame. Inspired by the decoupling strategy of identity features from the inputs [16], we develop an innovative end-to-end framework which strategically extracts identity-specific facial contours from temporally normalized frames, thereby reducing storage space and mitigating the negative impact of noise. Additionally, we design a novel fusion approach to integrate facial contour point information into physiological signal feature maps along the temporal dimension, enabling the model to gradually learn the relationship between facial contours and physiological signals. As shown in Fig 1, this approach steers the model’s focus to the facial contour region, ultimately improving its ability and interpretability to extract accurate physiological signals. Moreover, we employ an enhanced maximum magnitude multi-task loss to maintain a balance between the extraction of facial contours and BVP signals during the training. Extensive experiments are conducted on multiple benchmark datasets, demonstrating the rationality of our design and the superior performance than state-of-the-art methods in the heart rate estimation task.

To sum up, the main contributions of our work are three-fold as follows:

- We propose rFaceNet for physiological signal extraction. To the best of our knowledge, we are among the first to simultaneously extract facial contours and facial physiological signals, avoiding redundant inputs and unnecessary noise.
- We propose an innovative mechanism to integrate facial contour point information into physiological signal feature maps along the temporal dimension, which allows the model to focus on the facial contour and its interior.
- We use an enhanced maximum magnitude multi-task loss. After elaborate training, rFaceNet outperforms SOTA methods in several benchmark datasets for the heart rate estimation task.

2. RELATED WORK

In 2008, Verkruysse et al. [1] proposed a method for heart rate measurement using a home camera. Based on this research, more and more heart rate measurement methods based on rPPG technology were proposed. The traditional signal processing scheme [2–7] learned signals of different color channels through heuristics to explore the RGB images and reduced the effect of noise using techniques such as automatic face tracking and blind source separation. rPPG techniques were proven to efficiently restore the heart rate from video inputs. Non-end-to-end deep learning solutions were mainly used to improve the model learning efficiency by constructing spatio-temporal feature maps [8–12]. Meanwhile, end-to-end deep learning models were introduced into the rPPG domain [13–15, 18–22]. Existing techniques were sufficiently sophisticated in extracting heart rate estimates. However, increasingly complex preprocessing schemes and models introduced more non-interpretability and imposed more stringent requirements on the dataset. Some recent work [13–15] began to recognize the importance of facial appearance cues and enhanced the effectiveness and interpretability of the models by incorporating additional appearance inputs. However, attempts to extract facial contours from uniform temporal difference inputs have not emerged.

3. METHODOLOGY

In this section, we begin with an overall introduction to the rFaceNet framework in Sec 3.1. Then we provide a more detailed description of the Temporal Compressor Unit (TCU) in Sec 3.2, Cross-Task Feature Combiner (CTFC) in Sec 3.3. Finally, we show the multi-task loss function in Sec 3.4.

3.1. rFaceNet

Fig 2 shows an illustration of our rFaceNet, which is composed of two distinct branches. One branch is used to extract

facial contours from different identities and includes a temporal compression unit (Sec 3.2), a 2D feature extractor and an identity classifier. Note that the extraction of facial contours is implemented for different identities by means of the identity classifier. The other branch predicts BVP signals and includes a Cross-Task Feature Combiner (Sec 3.3), a 3D feature extractor and a BVP predictor.

3.2. Temporal Compressor Unit (TCU)

The Temporal Compressor Unit first shifts the dimensions of frames to move the spatio-temporal dimension to the end. Next, it compresses temporal dimension using 3D Adaptive Averaging Pooling while maintaining its original resolution. Lastly, it performs the dimensional compression transformation by converting it to a 2D tensor following the flatten operation. The TCU retains vital information, excluding temporal fluctuations, and enables the network to overlook minor fluctuations in the temporal field. Consequently, it maintains the identification of facial contours characteristic in a reduced dimension.

3.3. Cross-Task Feature Combiner (CTFC)

The Cross-Task Feature Combiner operates on the assumption that the pixel points representing physiological signals have minimal positional overlap with those of the facial profile used for identity recognition, and that the latter can surround the former in relative position.

As presented in Fig 2, the CTFC takes in the avg-identity feature map $FM_i^{H_i \times W_i}$ and rPPG feature map $FM_r^{H_r \times W_r \times T_r}$ from the 2D and 3D Feature Extractors. Firstly, the resolution of the avg-identity feature maps is adjusted to be consistent through up-sampling. The spatio-temporal dimensions of the identity feature map are then added and increased to match the shape of the rPPG feature map:

$$FM_i^{H_r \times W_r \times T_r} = \text{Cat}(FM_i^{H_r \times W_r}; \dots; FM_i^{H_r \times W_r}) \quad (1)$$

Pixel-points are then summed after two 1x1x1 convolutions that maintain the overall pixel ratios of each feature map unchanged. The outputs of the resulting Fusion Feature Map FuM are obtained.

$$FuM^{H_r \times W_r \times T_r} = \alpha \bullet FM_i + \beta \bullet FM_r \quad (2)$$

with α and β both scalars. The CTFC performs linear superposition of feature maps from different tasks by dimension adjustment and point-by-point convolution while preserving the original features. Fig 1 shows that our CTFC allows the rPPG extractor to focus its attention inside the contour through task-independent contour information.

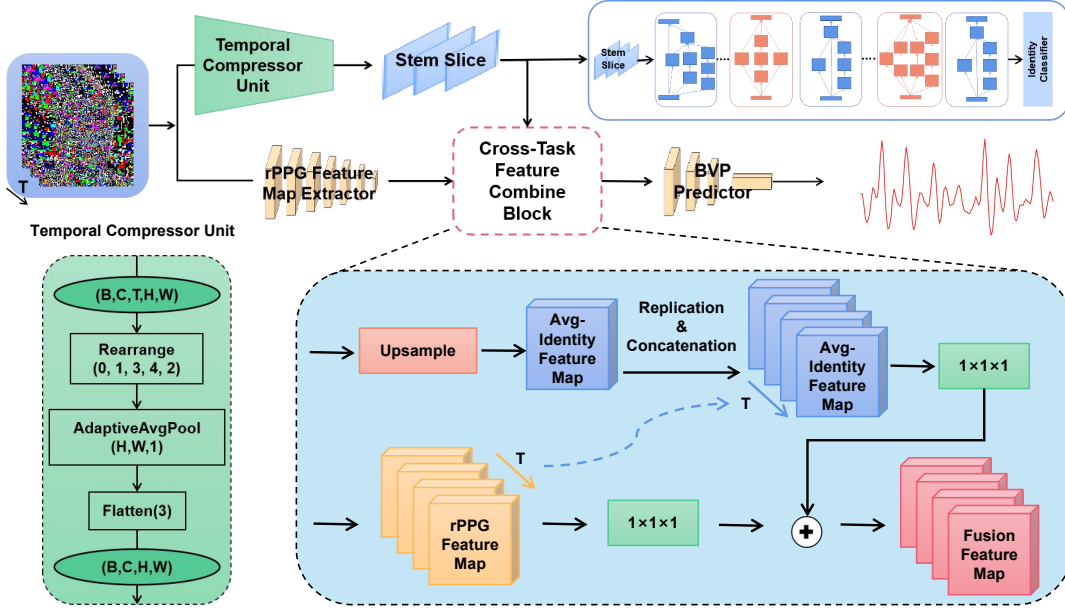


Fig. 2: The framework of rFaceNet, which uses temporally normalized frames as inputs. The Temporal Compressor Unit and the Cross-Task Feature Combiner are shown in detail.

3.4. Loss Function

Based on [23], a suitable multi-task loss function is employed for rFaceNet that maximizes the Gaussian likelihood with homologous uncertainty. To balance the two tasks of extracting identity-specific facial contours and computing BVP signals based on fingertip extraction, heart rate derived from fingertip-extracted BVP is incorporated into the design loss. ECG signals are avoided to prevent potential conflicts with the BVP signal extraction task. The heart rate is calculated as the frequency corresponding to the maximum peak in the power spectrum obtained after performing a Fourier transform on the BVP signals.

$$hr = \operatorname{argmax}_{freq(0.5 <, < 4.2)} (|FFT(bvp)|^2) \times 60 \quad (3)$$

In summary, it is assumed that the multiple outputs of the model consist of continuous outputs bvp , hr and discrete outputs id , modelled by Gaussian likelihood and soft maximum likelihood, respectively. The $Loss(W, \sigma_1, \sigma_2, \sigma_3)$ is as follows:

$$\begin{aligned} &= -\log p(bvp, hr, id = gt_{id} | f^W(x)) \\ &\approx \frac{1}{2\sigma_1^2} \|bvp - f^W(x)\|^2 + \log \sigma_1 \\ &\quad + \frac{1}{2\sigma_2^2} \|hr - f^W(x)\|^2 + \log \sigma_2 \\ &\quad + \frac{1}{\sigma_3} (-\log \operatorname{Softmax}(id, f^W(x))) + \log \sigma_3 \end{aligned} \quad (4)$$

And σ_1 , σ_2 and σ_3 are positive scalars. The loss function aims to balance the training for both regression and classifi-

cation tasks while preventing the premature learning of irrelevant information in the BVP signal prediction, which could otherwise result in significant fluctuations in the loss due to ambiguous identity information.

4. EXPERIMENTS

We first performed intra-dataset heart rate estimation experiment on the **VIPL-HR** [24] dataset. Then, to further demonstrate the validity of rFaceNet, we performed cross-dataset heart rate estimation experiments on the **UBFC-rPPG** [25] and **PURE** [26] datasets using recently released public benchmarks [27].

4.1. Datasets and Evaluations

The **VIPL-HR** database, designed for remote heart rate estimation from face videos, contains 2,378 VIS and 752 NIR videos from 107 subjects under various conditions. **UBFC-rPPG**, dedicated to rPPG analysis, includes 42 videos from 42 subjects without motion or lighting variations. **PURE** features recordings from 10 subjects (8 males, 2 females) across six movement conditions.

The heart rate estimation is evaluated on **VIPL-HR** using Standard Deviation (SD), Mean Absolute Error (MAE), Root Mean Square Error (RMSE), and Pearson's Correlation (ρ). For **UBFC-rPPG** and **PURE**, the rPPG-toolbox [27] is used to compare performance with existing methods, employing MAE, RMSE, and ρ as metrics.

Method	SD↓	MAE↓	RMSE↓	$\rho\uparrow$
Tulyakov2016▲ [2]	18.0	15.9	21.0	0.11
POS▲ [3]	15.3	11.5	17.2	0.30
CHROM▲ [5]	15.1	11.4	16.9	0.28
RhythmNet◆ [8]	8.11	5.30	8.14	0.76
ST-Attention◆ [9]	7.99	5.40	7.99	0.66
NAS-HR◆ [10]	8.10	5.12	8.01	0.79
CVD◆ [11]	7.92	5.02	7.97	0.79
Dual-GAN◆ [12]	7.63	4.93	7.68	0.81
I3D* [20]	15.9	12.0	15.9	0.07
PhysNet* [21]	14.9	10.8	14.8	0.20
DeepPhys* [13]	13.6	11.0	13.8	0.11
AutoHR* [22]	8.48	5.68	8.68	0.72
PhysFormer* [19]	7.74	4.97	7.79	0.78
PhysFormer+++* [18]	7.65	4.88	7.62	0.80
rFaceNet*	<u>4.87</u>	<u>5.21</u>	<u>7.13</u>	<u>0.87</u>

Table 1: Intra-dataset Heart Rate estimation in VIPL-HR. The symbols ▲, ◆, and * denote the traditional approach, the non-end-to-end learning based approach, and the end-to-end learning based approach, respectively. The best results are marked in **bold** and our results are underlined.

4.2. Implementation Details

Our method, implemented in Pytorch, uses MTCNN on the VIPL-HR dataset to crop and stabilize the face region, excluding head motion scenes (v2 and v9). The BVP and heart rate labels are upsampled to the original video sampling rate. During training, video frames are shaped into 64×128×128 segments, and following the approach suggested by [19], the frames are divided into 3-4 segments of approximately 8 seconds each for testing, averaging the segment heart rates for the video-level heart rate. It is worth noting that we only normalize the RGB video frame data, without additional data enhancement, and train rFaceNet with a batch size of 16 using the Adam optimizer (initial learning rate 1e-5, weight decay 5e-5).

To ensure fairness in benchmarking, the rppg-toolbox [27] is used for preprocessing, training, and evaluation in cross-dataset experiments. rFaceNet’s input size is set to 128×72×72, and the resolution is doubled by interpolation from the TCU module. The experiments are conducted on the UBFC-rPPG and PURE datasets, using the same hyperparameters as PhysNet. Our method ultimately achieves state-of-the-art results on both benchmarks, highlighting the effectiveness of our approach.

4.3. Intra-dataset Heart Rate Estimation

The table 1 illustrates that traditional methods often struggle with the VIPL-HR dataset due to complex environmental challenges. Deep learning models also face difficulties with weak physiological signals. However, our rFaceNet outperforms in heart rate estimation, leading in SD, RMSE, and ρ metrics by effectively leveraging facial contour informa-

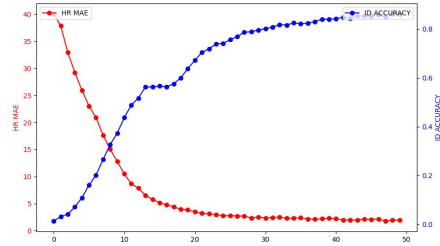


Fig. 3: MAE of HR Estimation vs. Accuracy of identification.

Train: PURE & Test: UBFC-rPPG			
Method	MAE↓	RMSE↓	$\rho\uparrow$
GREEN▲ [1]	19.73 ± 3.75	31.00 ± 235.38	0.37 ± 0.15
ICA▲ [4]	16.00 ± 3.09	25.65 ± 163.58	0.44 ± 0.14
CHROM▲ [5]	4.06 ± 1.21	8.83 ± 33.93	0.89 ± 0.07
LGI▲ [6]	15.80 ± 3.67	28.55 ± 236.17	0.36 ± 0.15
PBV▲ [7]	15.90 ± 3.25	26.40 ± 199.71	0.48 ± 0.14
POS▲ [3]	4.08 ± 1.01	7.72 ± 21.87	0.92 ± 0.06
TS-CAN* [14]	1.30 ± 0.40	2.87 ± 3.05	0.99 ± 0.02
PHYSNET* [21]	1.63 ± 0.53	3.79 ± 7.59	0.98 ± 0.03
DEEPPHYS* [13]	1.21 ± 0.41	2.90 ± 3.75	0.99 ± 0.02
EFF.PHYS-C* [15]	2.07 ± 0.92	6.32 ± 32.01	0.94 ± 0.05
rFaceNet*	<u>1.05 ± 0.35</u>	<u>2.51 ± 2.55</u>	<u>0.99 ± 0.02</u>
Train: UBFC-rPPG & Test: PURE			
Method	MAE↓	RMSE↓	$\rho\uparrow$
GREEN▲ [1]	10.09 ± 2.81	23.85 ± 217.81	0.34 ± 0.12
ICA▲ [4]	4.77 ± 2.08	16.07 ± 153.84	0.72 ± 0.09
CHROM▲ [5]	5.77 ± 1.79	14.93 ± 81.53	0.81 ± 0.08
LGI▲ [6]	4.61 ± 1.91	15.38 ± 134.14	0.77 ± 0.08
PBV▲ [7]	3.92 ± 1.61	12.99 ± 123.60	0.84 ± 0.07
POS▲ [3]	3.67 ± 1.46	11.82 ± 66.87	0.88 ± 0.06
TS-CAN* [14]	3.69 ± 1.74	13.8 ± 113.84	0.82 ± 0.08
PHYSNET* [21]	9.36 ± 2.39	20.63 ± 116.59	0.62 ± 0.10
DEEPPHYS* [13]	5.54 ± 2.30	18.51 ± 173.09	0.66 ± 0.10
EFF.PHYS-C* [15]	5.47 ± 2.10	17.04 ± 143.80	0.71 ± 0.09
rFaceNet*	<u>3.74 ± 1.52</u>	<u>11.95 ± 71.94</u>	<u>0.86 ± 0.07</u>

Table 2: Cross-dataset Heart Rate estimation in PURE and UBFC-rPPG.

tion. Despite being slightly behind in MAE, rFaceNet demonstrates robust performance in tracking heart rate trends under varying environmental conditions, proving its efficacy in complex scenarios. The learning curves of rFaceNet is also shown in Fig 3, visualizing the changes in MAE loss and facial contour-based identification accuracy for the heart rate estimation task during training. It is worth noting that the whole model first reaches an equilibrium point in the learning of the heart rate estimation task, which is then accompanied by a gradual convergence of the identification learning to the equilibrium and a synchronized fine-tuning of the heart rate estimation task.

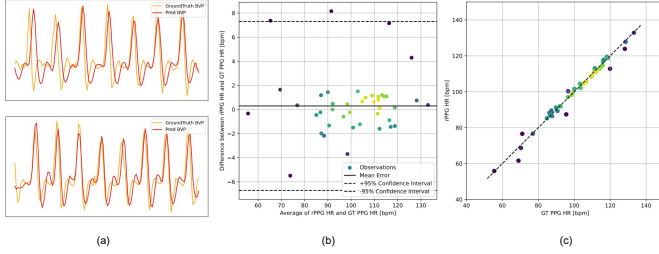


Fig. 4: Predicted Signals vs. GroundTruth Signals.

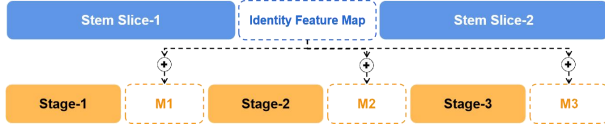


Fig. 5: Three fusion schemes in CTFC design.

4.4. Cross-dataset Heart Rate Estimation

As shown in Table 2, rFaceNet performs excellently in cross-dataset heart rate estimation tests. Particularly, when using the **UBFC-rPPG** as the test set, it achieves state-of-the-art results in MAE, RMSE, and ρ metrics. Similarly, when using **PURE** as the test set, rFaceNet maintains high accuracy, with only a slight difference from the optimal policy POS [3], outperforming all deep learning schemes. This may be attributed to the fact that the **UBFC-rPPG** dataset has fewer scenes, and models trained on it struggle with the six different motion scene transformations in the **PURE** dataset. Fig 4(a) shows that our extracted BVP signal closely matches the ground truth, especially in peak interval (heart rate) convergence, as reflected in the ρ metric in Table 1. Fig 4(b) presents a Bland-Altman plot comparing our method’s heart rate estimation with true heart rate values. The plot indicates that the difference between the two methods stays within 8 bpm in the $\pm 95\%$ confidence interval, demonstrating an acceptable level of agreement. Additionally, Fig 4(c) reveals a consistent pattern across a range of heart rate values, with most data points falling within the consistency range. This suggests that our method maintains accuracy across various heart rate values.

4.5. Ablation Study

In Table 3, the TCU and CTFC parts of rFaceNet are split to highlight the advantages of combining the two. When only the CTFC part is added, random noise of the same shape replace the avg-identity feature map inputs, achieving improved results. This demonstrates that adding noise can enhance model stability. On the other hand, adding only the TCU module results in rFaceNet having two parallel task branches that share a common input but do not interact, leading to a performance drop in heart rate estimation due to the need to balance the training speeds of the two tasks. To experiment with the

TCU	CTFC	MAE↓	RMSE↓	ρ ↑
×	×	1.99 ± 0.82	5.67 ± 24.84	0.95 ± 0.05
	✓	1.57 ± 0.46	3.37 ± 4.17	0.98 ± 0.03
	×	2.53 ± 0.88	6.26 ± 26.27	0.94 ± 0.05
✓	Stage-1	2.22 ± 0.91	6.30 ± 25.15	0.94 ± 0.06
	Stage-2	1.26 ± 0.43	3.04 ± 3.88	0.99 ± 0.03
	Stage-3	1.05 ± 0.35	2.51 ± 2.55	0.99 ± 0.02

Table 3: Ablations of TCU and CTFC.

optimal design of the CTFC module, three fusion schemes are tested corresponding to the output feature maps M1, M2, and M3 from three stages of BVP signal extraction (stage 1, stage 2, and stage 3). As shown in Fig 5, M1 has a resolution size of $\lfloor H^{input}/2, W^{input}/2 \rfloor$, M2 has a resolution size of $\lfloor H^{input}/4, W^{input}/4 \rfloor$, and M3 has a resolution size of $\lfloor H^{input}/8, W^{input}/8 \rfloor$.

According to Table 3, the adding CTFC to the output M3 of Stage-3 yield optimal results. Fusion at the early stage of BVP signal extraction leads to decreased accuracy, possibly due to model instability during initial learning and increased noise from identity feature fusion at that stage. As demonstrated in Table 3, our design proves superior, achieving optimal results when both components are combined.

5. CONCLUSIONS

In summary, our study introduces rFaceNet, a novel rPPG method that innovatively combines a Temporal Compressor Unit (TCU) to extract facial contours from temporally normalized frame inputs, thereby reducing redundant data. Additionally, we integrate a Cross-Task Feature Combiner (CTFC) to assimilate facial contour point information along the time dimension into physiological signal feature maps. This enhances the model’s focus on pertinent facial regions, thereby improving the validity and interpretability of BVP signals extracted by rPPG. We demonstrate rFaceNet’s superior performance in various benchmark tests. Furthermore, our study does not explore the potential integration of this mechanism with face recognition systems, which represents a promising direction for future research.

6. REFERENCES

- [1] Wim Verkruyse, Lars O Svaasand, and J Stuart Nelson, “Remote plethysmographic imaging using ambient light,” *Optics express*, vol. 16, no. 26, pp. 21434–21445, 2008.
- [2] Sergey Tulyakov, Xavier Alameda-Pineda, Elisa Ricci, Lijun Yin, Jeffrey F Cohn, and Nicu Sebe, “Self-adaptive matrix completion for heart rate estimation from face videos under realistic conditions,” in *CVPR*, 2016, pp. 2396–2404.
- [3] Wenjin Wang, Albertus C Den Brinker, Sander Stuijk, and Gerard De Haan, “Algorithmic principles of remote

- ppg,” *IEEE Transactions on Biomedical Engineering*, vol. 64, no. 7, pp. 1479–1491, 2016.
- [4] Ming-Zher Poh, Daniel J McDuff, and Rosalind W Picard, “Advancements in noncontact, multiparameter physiological measurements using a webcam,” *IEEE transactions on biomedical engineering*, vol. 58, no. 1, pp. 7–11, 2010.
 - [5] Gerard De Haan and Vincent Jeanne, “Robust pulse rate from chrominance-based rppg,” *IEEE Transactions on Biomedical Engineering*, vol. 60, no. 10, pp. 2878–2886, 2013.
 - [6] Christian S Pilz, Sebastian Zauneder, Jarek Krajewski, and Vladimir Blazek, “Local group invariance for heart rate estimation from face videos in the wild,” in *CVPR*, 2018, pp. 1254–1262.
 - [7] Gerard De Haan and Arno Van Leest, “Improved motion robustness of remote-ppg by using the blood volume pulse signature,” *Physiological measurement*, vol. 35, no. 9, pp. 1913, 2014.
 - [8] Xuesong Niu, Shiguang Shan, Hu Han, and Xilin Chen, “Rhythmnet: End-to-end heart rate estimation from face via spatial-temporal representation,” *TIP*, vol. 29, pp. 2409–2423, 2019.
 - [9] Xuesong Niu, Xingyuan Zhao, Hu Han, Abhijit Das, Antitza Dantcheva, Shiguang Shan, and Xilin Chen, “Robust remote heart rate estimation from face utilizing spatial-temporal attention,” in *FG 2019*. IEEE, 2019, pp. 1–8.
 - [10] Hao Lu and Hu Han, “Nas-hr: Neural architecture search for heart rate estimation from face videos,” *Virtual Reality & Intelligent Hardware*, vol. 3, no. 1, pp. 33–42, 2021.
 - [11] Xuesong Niu, Zitong Yu, Hu Han, Xiaobai Li, Shiguang Shan, and Guoying Zhao, “Video-based remote physiological measurement via cross-verified feature disentangling,” in *ECCV 2020*. Springer, 2020, pp. 295–310.
 - [12] Hao Lu, Hu Han, and S Kevin Zhou, “Dual-gan: Joint bvp and noise modeling for remote physiological measurement,” in *CVPR*, 2021, pp. 12404–12413.
 - [13] Weixuan Chen and Daniel McDuff, “Deepphys: Video-based physiological measurement using convolutional attention networks,” in *ECCV*, 2018, pp. 349–365.
 - [14] Xin Liu, Josh Fromm, Shwetak Patel, and Daniel McDuff, “Multi-task temporal shift attention networks for on-device contactless vitals measurement,” *Advances in Neural Information Processing Systems*, vol. 33, pp. 19400–19411, 2020.
 - [15] Xin Liu, Brian Hill, Ziheng Jiang, Shwetak Patel, and Daniel McDuff, “Efficientphys: Enabling simple, fast and accurate camera-based cardiac measurement,” in *IEEE/CVF winter conference on applications of computer vision*, 2023, pp. 5008–5017.
 - [16] Wei-Hao Chung, Cheng-Ju Hsieh, Sheng-Hung Liu, and Chiou-Ting Hsu, “Domain generalized rppg network: Disentangled feature learning with domain permutation and domain augmentation,” in *ACCV*, 2022, pp. 807–823.
 - [17] Ramprasaath R Selvaraju, Michael Cogswell, Abhishek Das, Ramakrishna Vedantam, Devi Parikh, and Dhruv Batra, “Grad-cam: Visual explanations from deep networks via gradient-based localization,” in *ICCV*, 2017, pp. 618–626.
 - [18] Zitong Yu, Yuming Shen, Jingang Shi, Hengshuang Zhao, Yawen Cui, Jiehua Zhang, Philip Torr, and Guoying Zhao, “Physformer++: Facial video-based physiological measurement with slowfast temporal difference transformer,” *International Journal of Computer Vision*, vol. 131, no. 6, pp. 1307–1330, 2023.
 - [19] Zitong Yu, Yuming Shen, Jingang Shi, Hengshuang Zhao, Philip HS Torr, and Guoying Zhao, “Physformer: Facial video-based physiological measurement with temporal difference transformer,” in *CVPR*, 2022, pp. 4186–4196.
 - [20] Joao Carreira and Andrew Zisserman, “Quo vadis, action recognition? a new model and the kinetics dataset,” in *CVPR*, 2017, pp. 6299–6308.
 - [21] Zitong Yu, Xiaobai Li, and Guoying Zhao, “Remote photoplethysmograph signal measurement from facial videos using spatio-temporal networks,” *arXiv preprint arXiv:1905.02419*, 2019.
 - [22] Zitong Yu, Xiaobai Li, Xuesong Niu, Jingang Shi, and Guoying Zhao, “Autohr: A strong end-to-end baseline for remote heart rate measurement with neural searching,” *IEEE Signal Processing Letters*, vol. 27, pp. 1245–1249, 2020.
 - [23] Alex Kendall, Yarin Gal, and Roberto Cipolla, “Multi-task learning using uncertainty to weigh losses for scene geometry and semantics,” in *CVPR*, 2018, pp. 7482–7491.
 - [24] Xuesong Niu, Hu Han, Shiguang Shan, and Xilin Chen, “Vipl-hr: A multi-modal database for pulse estimation from less-constrained face video,” in *ACCV 2018*. Springer, 2019, pp. 562–576.
 - [25] Serge Bobbia, Richard Macwan, Yannick Benezeth, Alamin Mansouri, and Julien Dubois, “Unsupervised skin tissue segmentation for remote photoplethysmography,” *Pattern Recognition Letters*, vol. 124, pp. 82–90, 2019.
 - [26] Ronny Stricker, Steffen Müller, and Horst-Michael Gross, “Non-contact video-based pulse rate measurement on a mobile service robot,” in *The 23rd IEEE International Symposium on Robot and Human Interactive Communication*. IEEE, 2014, pp. 1056–1062.
 - [27] Xin Liu, Girish Narayanswamy, Akshay Paruchuri, Xiaoyu Zhang, Jiankai Tang, Yuzhe Zhang, Yuntao Wang, Soumyadip Sengupta, Shwetak Patel, and Daniel McDuff, “rppg-toolbox: Deep remote ppg toolbox,” *arXiv preprint arXiv:2210.00716*, vol. 6, pp. 13, 2022.